JACS
JOURNAL OF THE AMERICAN CHEMICAL SOCIETY
Article
Cite This: J. Am. Chem. Soc. XXXX, XXX, XXX−XXX
pubs.acs.org/JACS

Pathway Dependence in the Fuel-Driven Dissipative Self-Assembly of Nanoparticles

Raphael K. Grötsch,[†] Caren Wanzke,[†] Maximilian Speckbacher,[‡] Arzu Angı,[†,⊥] Bernhard Rieger,[†,⊥] and Job Boekhoven*[,†,∥]

[†]Department of Chemistry and [∥]Institute for Advanced Study, Technical University of Munich, Lichtenbergstraße 4, 85748 Garching, Germany

[‡]Molecular Electronics, Department of Electrical and Computer Engineering, Technical University of Munich, Thersienstraße 90, 80333 Munich, Germany

[⊥]Wacker-Chair of Macromolecular Chemistry, Catalysis Research Center, Ernst-Otto-Fischer-Straße 1, 85747 Garching, Germany

Supporting Information

ABSTRACT: We describe the self-assembly of gold and iron oxide nanoparticles regulated by a chemical reaction cycle that hydrolyzes a carbodiimide-based fuel. In a reaction with the chemical fuel, the nanoparticles are chemically activated to a state that favors assembling into clusters. The activated state is metastable and decays to the original precursor reversing the assembly. The dynamic interplay of activation and deactivation results in a material of which the behavior is regulated by the amount of fuel added to the system; they either did not assemble, assembled transiently, or assembled permanently in kinetically trapped clusters. Because of the irreversibility of the kinetically trapped clusters, we found that the behavior of the self-assembly was prone to hysteresis effects. The final state of the system in the energy landscape depended on the pathway of preparation. For example, when a large amount of fuel was added at once, the material would end up kinetically trapped in a local minimum. When the same amount of fuel was added in small batches with sufficient time for the system to re-equilibrate, the final state would be the global minimum. A better understanding of pathway complexity in the energy landscape is crucial for the development of fuel-driven supramolecular materials.

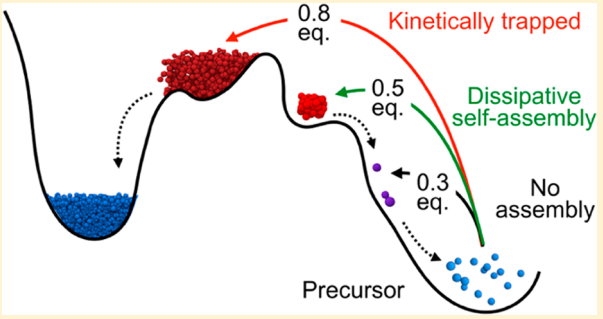

Downloaded by Job Boekhoven at 00:36:59:831 on June 17, 2019
from https://pubs.acs.org/doi/10.1021/jacs.9b02004.

INTRODUCTION

In supramolecular materials, molecules or nanoparticles assemble into larger, more complex structures.[1−4] The building blocks in these assemblies are held together by noncovalent interactions, which result in materials that have vastly different properties compared to their nonassembled building blocks. Particularly successful examples of building blocks include amphiphiles,[5] gelators,[6] peptides,[7] and nanoparticles functionalized with DNA.[8] The type of assembly and its associated material properties can be encoded in the molecular design of the building blocks, resulting in exciting materials like supramolecular polymers that can regulate cell behavior.[9−11] However, recent work has demonstrated that the intended self-assembled state is sometimes not reached, because the assemblies can trap molecules in a local minimum in their energy landscape.[12−14] Such systems are prone to hysteresis effects, which means that the order in which the assembly is prepared can affect the final state. Even if the composition of the final material is the same, its material properties can differ depending on the preparative pathway.[15−18] The properties of supramolecular materials are thus not only dependent on the molecular design of the building blocks but can also depend on the pathway of preparation of the materials.

In dissipative self-assembly, the self-assembly of molecules or nanoparticles is regulated by a chemical reaction cycle.[19−21] The reaction cycle comprises a fuel-driven activation reaction and a spontaneous deactivation reaction. In the activation reaction, a precursor reacts irreversibly with a chemical fuel giving rise to a building block for self-assembly. The deactivation reaction spontaneously reverts the building block to the precursor. The consequence of the reaction cycle is that building blocks have a finite lifetime. The finite lifetime of the building blocks in the assemblies means that the assemblies are dynamic[22−24] and evolve. The emerging material properties are controlled by kinetic parameters, like the initial concentration of fuel[25] and feedback of the assemblies on their reaction cycle,[26,27] which leads to exciting materials like self-abolishing supramolecular gels,[22,28] self-erasing inks,[29] solutions of supramolecular polymers that oscillate between morphologies,[30] and solutions of nano-

Received: February 27, 2019
Published: June 3, 2019

© XXXX American Chemical Society

DOI: 10.1021/jacs.9b02004
J. Am. Chem. Soc. XXXX, XXX, XXX−XXX

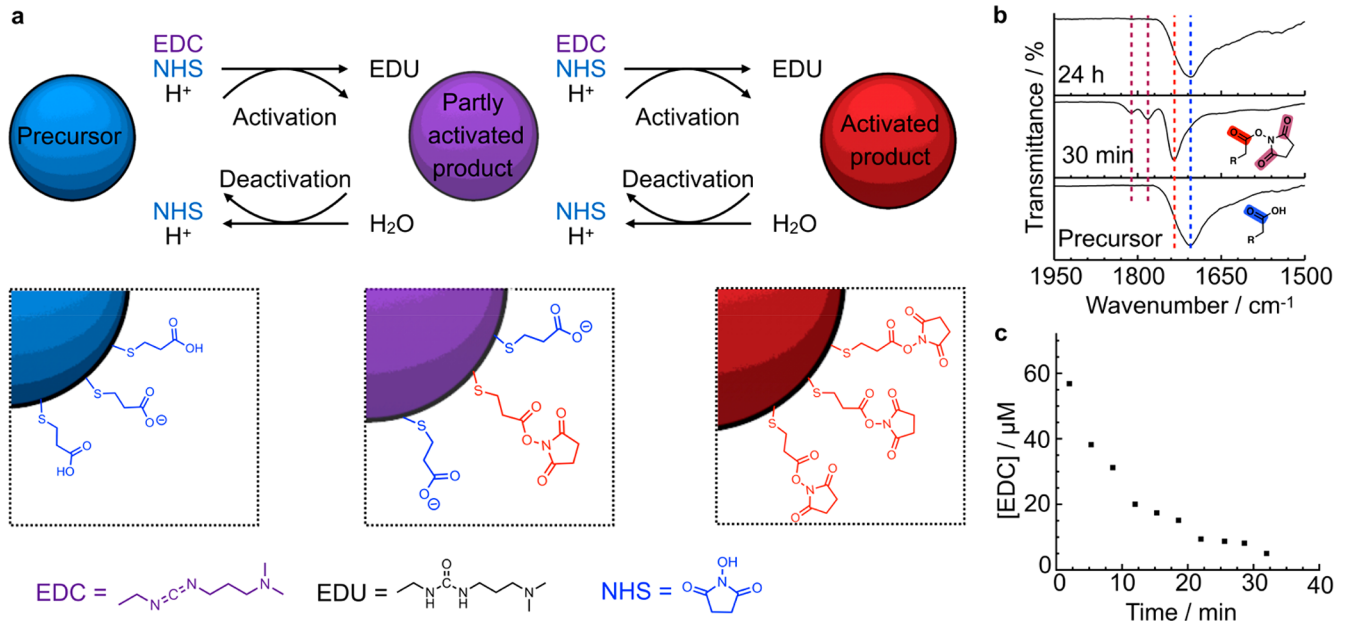

Figure 1. (a) The chemical reaction cycle driven by the hydrolysis of EDC. The carboxylates on a gold nanoparticle can react with EDC and NHS to form the corresponding NHS ester (activation). The intrinsically unstable NHS-ester deactivates over time into the precursor via its hydrolysis. Depending on the amount of EDC added, the precursor is partly or fully activated. (b) FTIR spectra of the nanoparticles before and 30 min and 24 h after the addition of 0.5 equiv (125 μM) of EDC to a solution of the precursor. Dashed lines from purple to blue mark the peaks for 1811, 1782, 1734, and 1705 cm^{-1}. (c) The EDC concentration as a function of time for the same experimental condition as described in (b).

particles clusters that degrade over time.[31−33] Despite these exciting material properties, fundamental understanding of the energy landscapes and evolving material properties of fuel-driven dissipative self-assembly, in particular, in the context of pathway complexity, is lacking.

RESULTS AND DISCUSSION

In this work, we describe that pathway dependence is also applicable to dissipative self-assembly. We use gold and iron oxide nanoparticles as precursors in a chemical reaction cycle. The hydrolysis of condensing agents drives the reaction cycle. Upon activation, the nanoparticles can either remain unassembled, assemble into transient clusters, or form a kinetically trapped assembly, depending on the amount of fuel added. However, we also find that the same amount of fuel can result in a different response depending on the chosen preparative pathway.

As building blocks, we used carboxylate-terminated gold or iron oxide nanoparticles with a diameter of 3.5 and 15 nm, respectively, as measured by cryogenic transmission electron microscopy (see Materials and Methods in Supporting Information and Figure SI1). These nanoparticles were well-soluble in water, and we regulated their assembly behavior by a chemical reaction cycle we recently introduced (Figure 1a).[31] In the reaction cycle, the carboxylate groups on the particles were transiently converted in their corresponding *N*-hydroxysuccinimide (NHS) ester driven by the hydrolysis of 1-ethyl-3-(3-(dimethylamino)propyl)-carbodiimide (EDC). In the activation reaction, the EDC reacted irreversibly with the surface-bound carboxylic acid groups and NHS in the solution to form the corresponding metastable NHS-ester. In the deactivation, the NHS-ester hydrolyzed to the original carboxylic acid state. In the buffer at pH 6.4, the carboxylic acids on the nanoparticles in solution were to some degree deprotonated rendering them well-soluble in water. In contrast, the NHS-ester is uncharged, and the loss of charge was expected to induce the clustering of the particles, thereby inducing the dissipative self-assembly of the nanoparticles.

We assessed the behavior of the gold nanoparticles in response to EDC by Fourier transformed infrared (FTIR) spectroscopy. We prepared a solution of the nanoparticles at a concentration of 250 μM acid groups (Figure SI2) in 25 mM NHS and 20 mM 2-(*N*-morpholino)ethanesulfonic acid (MES) buffer at pH 6.4, which yielded a reddish solution. We consider the concentration of 250 μM acid groups as 1 equiv when calculating the amount of EDC we added to initiate the reaction cycle. In other words, 1.0 equiv of EDC could theoretically convert all acid groups on the particles into their corresponding NHS-ester. On the basis of the diameter of the gold nanoparticles and assuming a surface area per mercaptopropionic acid of 0.16 nm^2,[34] we calculated that, on average, each particle carries 250 molecules of mercaptopropionic acid (see Methods section in Supporting Information). The FTIR spectroscopy on the particles before the addition of EDC revealed a clear band associated with the carbonyl of a carboxylic acid (Figure 1b). We added 0.5 equiv of EDC (125 μM) to the precursor solution to initiate the reaction cycle and observed the formation of three new bands, which we associated with the carbonyls of the NHS-ester. After 24 h, FTIR showed that the three new bands had disappeared. In other words, the spectrum was similar to the spectrum of the precursor. Similar trends in the FTIR data were found when 0.3 equiv (75 μM) or 0.8 equiv (200 μM) of EDC was added to the solutions (vide infra, Figure SI3).

We used high-pressure liquid chromatography (HPLC) to follow the evolution of the concentration of EDC during the reaction cycle. We found a sharp decay of the concentration of EDC in the first minute, which we explain by a previously described side reaction between EDC and NHS.[35] We found a further decline in the EDC concentration over time, which is

DOI: 10.1021/jacs.9b02004
J. Am. Chem. Soc. XXXX, XXX, XXX−XXX

the result of the reaction of the carboxylic acid groups on the surface of the particles with the EDC (Figure 1c). After 30 min, most of the EDC had been consumed by the reaction cycle. The combination of FTIR and HPLC analytics show strong evidence for the chemical reaction cycle described in Figure 1a.

Characterizing the macroscopic behavior of the nanoparticle solution upon the addition of EDC was the next step. In a first experiment, the precursor was fueled with 0.3, 0.5, or 0.8 equiv of EDC. By time-lapse photography, no apparent changes were visible in the first 30 min for any of the samples. However, as time progressed, the solution fueled with 0.8 equiv of EDC showed the formation of a precipitate, while the supernatant became clear (Figure 2a). We followed the evolution of the

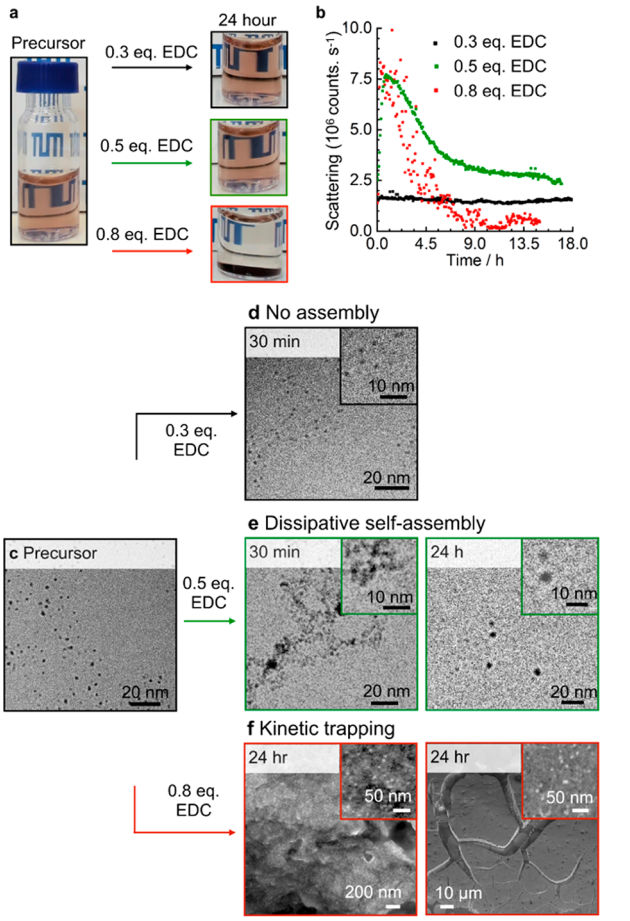

Figure 2. (a) Photographs of the solutions before (precursor) and 24 h after EDC addition. (b) The scattering rates as measured by DLS as a function of time for different amounts of EDC added to the nanoparticles. (c–e) Cryo-TEM micrographs of the precursor solution, a solution 30 min after fueling with 0.3 equiv of EDC (d) and a solution 30 min and 24 h after fueling with 0.5 equiv of EDC. (f) SEM micrographs of the precipitate formed by fueling the precursor with 0.8 equiv of EDC.

material in more detail using dynamic light scattering (DLS). We measured that the particles had a hydrodynamic diameter of 13 nm before the addition of EDC. With 0.3 equiv of EDC, we did not observe any evidence of self-assembly by DLS. That means, neither the size of the particles nor the total scattering rate was affected by the addition of EDC (Figures 2b and SI4). The lack of assemblies is a strong indication that an insufficient amount of NHS-ester per particle is formed to overcome the interparticle repulsion, and thus no assembly was induced. In contrast, when we added 0.5 equiv of EDC, the scattering rate increased from 2 to 7.5 Mcps, while the mean hydrodynamic diameter of the particle in solution increased from 13 to 41 nm in the first hour (Figure SI4). After 2 h, the scattering decreased gradually to a value close to the original level. In that time frame, the radius had also decreased to the original 12 nm. These combined experiments suggest that we can induce transient self-assembly of the gold nanoparticles provided that a sufficient amount of EDC is added. When the nanoparticles were fueled by 0.8 equiv of EDC, DLS showed a similar rapid increase in the size and scattering rate, pointing toward the assembly of the particles. However, the scattering rate as a function of time became noisy, and the radius could not be fitted reliably. The scattering rate dropped to a level far below the original value after 6 h and never came back to the original level. We explain the loss of scattering to the precipitation of the gold nanoparticles in line with the observations made by time-lapse photography.

To confirm that the self-assembly was driven by the hydrophobization upon forming the NHS-ester, we performed two control experiments with DLS. These experiments rule out, for example, that the intermediate *O*-acylisourea[35] was causing the agglomeration. First, we exchanged the NHS in solution for the anionic *N*-hydroxysulfosuccinimide (sulfo-NHS) and fueled the experiment with 0.5 equiv of EDC. In this experiment, DLS showed no evidence of self-assembly. In a second experiment, no NHS was present when we fueled with 0.5 equiv of EDC. Again, DLS showed no evidence of assembly. Both experiments demonstrate that the hydrophobic NHS is required to induce assembly (Figure SI5).

We used electron microscopy to analyze the assembly of the gold nanoparticles induced by EDC. Before the cycle was initiated, cryo-TEM showed individual nanoparticles and small aggregates of the nanoparticles (Figure 2c). When the solution was imaged 30 min after the addition of 0.3 equiv of EDC, we found a similar scenario, that is, predominantly nonassembled nanoparticles (Figure 2d). In contrast, when we added 0.5 equiv of EDC as fuel, we found clusters of the particles. These clusters comprised hundreds of particles that were relatively loosely packed (Figures 2e and SI6). Moreover, after 24 h the clusters were not observed, but instead, mostly individual nanoparticles were found reminiscent of the precursor state. The electron microscopy data, combined with the DLS data and the study on the kinetics of the reaction cycle, provide compelling data to conclude that we can induce the transient dissipative assembly of gold nanoparticles under these conditions.

In contrast, when we investigated the sample that was fueled with 0.8 equiv of EDC by scanning electron microscopy (SEM), we observed assemblies of several hundreds of micrometers (Figure 2f). We tried cryo-TEM imaging, but because of the size of the clusters, it was not possible. These large assemblies consisted of thousands of nanoparticles. The size of these assemblies explains why they precipitated. Moreover, the size could also explain why, after 24 h, the structures had not disassembled. Samples stored for four weeks also showed the precipitation (Figure SI7), which seems to suggest that the precipitate traps the particles into an assembly from which they cannot escape.

The nanoparticles could be kinetically trapped because of two reasons. Either the nanoparticles are densely packed and

DOI: 10.1021/jacs.9b02004
J. Am. Chem. Soc. XXXX, XXX, XXX–XXX

exclude all the water from the assemblies, which inhibits the hydrolysis (deactivation) reaction and, thus, inhibits the disassembly. We found a similar mechanism of inhibition of hydrolysis in other work.[36] Alternatively, because of the relatively high fuel concentration, the particles form a large assembly and can undergo strong noncovalent interactions (e.g., hydrogen bonding of the carboxylic acids or van der Waals interactions), such that the energy barrier for disassembly becomes too high to overcome. Such kinetic trapping of nanoparticles, even in their deactivated state, has been demonstrated before for gold nanoparticles that self-assembled in response to light.[37]

To test the first hypothesis, we performed an FTIR study on the assemblies after addition of 0.8 equiv of EDC and tested whether the surface of the nanoparticles reverted to their original state. For these clusters, NHS-ester bands could be measured after 24 h (Figure 3a; Figure SI8 for full spectra).

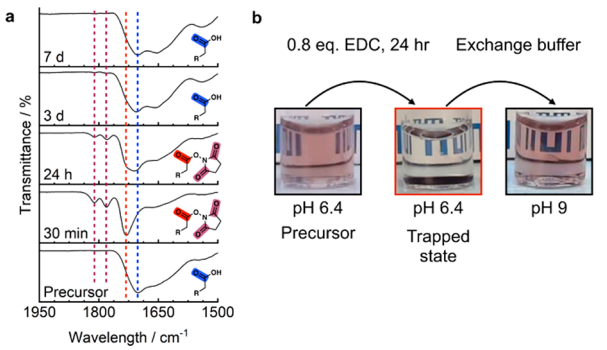

Figure 3. (a) FTIR analyses of the sample fueled with 0.8 equiv of EDC over time. (b) Photographs before and 24 h after the addition of 0.8 equiv of EDC. Only by addition of buffer at pH 9 could the nanoparticles be redissolved.

That seems to suggest that hydrolysis is delayed, because these bands were not visible after 24 h in the dissipative self-assembling sample (vide supra, Figure 1b). However, 7 d after addition of the 0.8 equiv of EDC, the FTIR showed that the NHS ester had fully hydrolyzed and that the precursor state was recovered from a surface chemistry point of view. Nevertheless, the deactivated nanoparticles remained in a precipitate. The combined observation seems to suggest that both hypothesized mechanisms play a role: the large scale of the assemblies slows the hydrolysis but does not inhibit it entirely, and the large assemblies kinetically trap the nanoparticles, whether they are in the activated state or not.

We found that samples fueled with more than 0.8 equiv of EDC behaved similarly; that is, all samples resulted in a precipitate that did not dissolve (Figure SI9). Vigorously shaking, sonicating or heating these samples did not bring the precipitated nanoparticles back to their precursor state. Only by increasing the pH from 6.4 to 9.0 by exchanging the buffer could we redissolve the precipitate (Figure 3b). This observation also confirms that the particles are trapped by noncovalent reversible interactions, which can be overcome by increasing the interparticle electrostatic repulsion.[38] Indeed, a final electron microscopy study demonstrated that the particles, before initiating the cycle and after 24 h in the kinetically trapped state, had similar diameters as measured by conventional TEM (Figure SI10). Because the kinetically trapped clusters were large, we chose to use conventional TEM over cryo-TEM in this experiment. That observation rules out that the particles coalesced when trapped in the precipitate. Taken together, the precipitate comprised the particles that were kinetically trapped due to noncovalent interactions.

The combined data set allows us to sketch an overview of the pathways and energy landscapes involved in the fuel-driven self-assembly of the nanoparticles (Figure 4). In the reaction

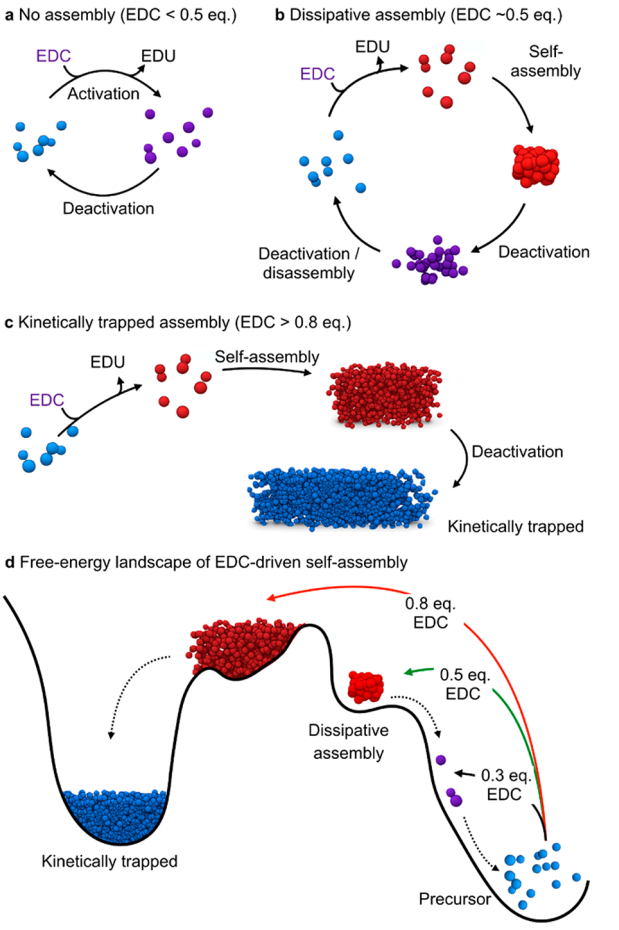

Figure 4. Pathways of self-assembly driven by a chemical reaction cycle. (a) The nonassembling cycle. (b) The dissipative self-assembling cycle. (c) The pathway that was resulting in kinetically trapped particles. (d) Schematic representation of the free energy landscape of the EDC driven self-assembly. Solid lines are uphill events that consume energy. Dashed lines are spontaneous downhill events. Note that there is no pathway from the kinetically trapped state to the precursor state.

pathways, there is a minimum amount of fuel required to induce the self-assembly of the activated state; that is, when 0.3 equiv or less of EDC was used, we observed the NHS-ester but no evidence for self-assembly. We refer to this as the nonassembling pathway (Figure 4a). In contrast, when 0.5 equiv of fuel was added, the reaction cycle formed particles that were sufficiently activated to induce their self-assembly. The particles disassembled over time, which was driven by the deactivation reaction. We refer to this as the dissipative self-assembly pathway; that is, the particles transiently assemble by dissipating energy obtained from the reaction cycle (Figure 4b). Finally, when more than 0.5 equiv of fuel was added, the particles were sufficiently activated for assembly. However, they assembled in a tightly clustered state that inhibited deactivation to some degree. Moreover, after deactivation, the

DOI: 10.1021/jacs.9b02004
J. Am. Chem. Soc. XXXX, XXX, XXX−XXX

particles remained kinetically trapped in the large assemblies (Figure 4c).

In Figure 4d, we depict a tentative energy landscape of the self-assembly of the nanoparticles driven by EDC. The precursor state (right) is likely the global minimum of the landscape. When EDC (energy) is added, the population can shift uphill. For example, when 0.3 equiv is added (non-assembling pathway), the particles are activated but freely fall back to the precursor state over time. When 0.5 equiv is added, the particles are further activated and can assemble. That nonequilibrium state represents a local minimum in the landscape. Its low energy barrier ensures that the particles can disassemble over time. Finally, when 0.8 equiv of fuel is added, the particle reaches another local minimum. This minimum is characterized by a high-energy barrier toward the precursor state. Instead, after deactivation, the state remains kinetically trapped in a final local minimum.

While the dissipative self-assembly of nanoparticles driven by various chemical reaction cycles has been demonstrated before,[29,32,39] the notion of kinetically trapping has been underexplored.[37] To test if the fuel-driven self-assembly and kinetic trapping that we described in this work is unique to one precursor, we tested the chemical reaction cycle to drive the self-assembly of carboxylate-terminated iron oxide nanoparticles. We used commercially available nanoparticles with a diameter of 15 ± 2 nm as measured by cryo-TEM (see Figure SI1) and a hydrodynamic diameter of 28 ± 7 nm as measured by DLS (Table SI1). Besides the fact that these particles are based on a different metal, they also carry a different surface chemistry. The iron oxide particles were covered with a monolayer of oleic acid, which was then coassembled with hydrolyzed poly(maleic anhydride-*alt*-1-octadecene). The concentration of surface-bound carboxylates was 5 mM in a buffer of 200 mM MES at pH 6.5 and 20 mM NHS. We considered the concentration of 5 mM acid groups as 1 equiv when calculating the equivalents of EDC to add. In line with the previous observations, the behavior of the solution depended on the amount of EDC we added. For the addition of 0.4 equiv of EDC (2.0 mM), no change by time-lapsed photography or by DLS was detected (Figure 5a,b). In contrast, when we added 2.0 equiv of EDC (10 mM), we observed precipitation of the iron oxide nanoparticles. DLS showed a rapid increase in the scattering rate after which it decayed to zero. These observations are in line with the kinetic trapping scenario observed for the gold nanoparticles. We used IR spectroscopy to confirm the transient formation of the NHS-ester. When 0.4 or 2.0 equiv of EDC was added, we observed the peaks characteristic for the NHS ester. Moreover, for 0.4 equiv, the peaks were not visible within 24 h. In contrast, for 2.0 equiv, it took 3 d to show similar bands as before the addition of EDC (Figures 5c,d and SI11 for full spectra). The combined data sets suggest that the behavior of the EDC-driven chemical reaction cycle is similar for gold and iron oxide nanoparticles that carry a carboxylate group on their surface.

The notion that two of the EDC-driven pathways were reversible (nonassembling and dissipative assembling) and a third pathway was not (kinetically trapped) prompted us to explore pathway complexity experiments, that is, an experiment in which the pathway to the same final conditions leads to different outcomes. We compared the outcome of two experiments that both received more than the 0.8 equiv of fuel. In one experiment, we added the fuel in small batches of less than 0.5 equiv. In the other experiment, we added all fuel at once.

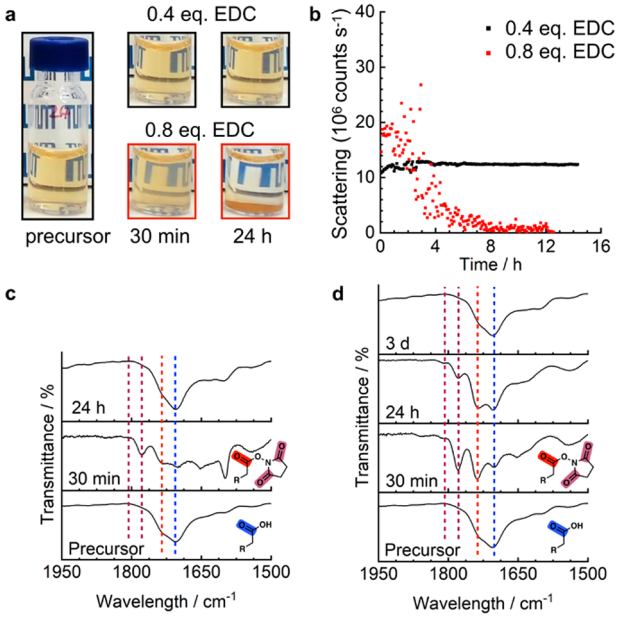

Figure 5. (a) Photographs of the iron oxide nanoparticle solutions before (precursor), 30 min, and 24 h after EDC addition. (b) The scattering rates as measured by DLS as a function of time for different amounts of EDC added to the nanoparticles. (c, d) FTIR diagram of the precursor, 30 min and 24 h after addition of 0.4 (c) and 0.8 (d) equiv of EDC to a solution of the precursor. Dashed lines from purple to blue mark the peaks for 1811, 1782, 1734, and 1705 cm^{-1}.

Specifically, we added three batches of 0.3 equiv of EDC at 24 h intervals to the gold nanoparticles. In another experiment, we added two batches of 0.45 equiv of EDC with 36 h intervals. In a final experiment, we added 0.9 equiv in one batch and waited for 72 h (Figure 6a). The multiple additions of smaller batches of fuel resulted in a solution of the nanoparticles with no evidence of precipitation over the entire course of the experiment. In contrast, when the 0.9 equiv were added to the nanoparticles in one batch, the experiment resulted in precipitation. After 72 h, all solutions were measured by DLS spectroscopy, which showed similar diameter and count rates as the precursor sample for the first two samples. In contrast, the sample fueled with 0.9 equiv of fuel showed a greater radius and a lower count rate, confirming the kinetically trapped state (see Table SI2).

We added to the iron oxide nanoparticles five batches of 0.4 equiv of EDC with two-day intervals, as well as 2.0 equiv in one batch (Figure 6b). While no precipitation was observed for the sequentially fueled sample, the other sample resulted in the formation of a precipitate within hours after addition of the fuel, which remained present during the entire experiment. DLS spectroscopy confirmed that the sequentially fueled sample showed similar scattering rate and particle diameter compared to the precursor. In contrast, the sample that received the same amount of fuel, but all at once, showed no reliable scattering data, indicative of the kinetically trapped precipitate (see Table SI2).

CONCLUSIONS

Our work shows that the self-assembly behavior of gold and iron oxide nanoparticles can be regulated by an EDC-driven chemical reaction cycle that converts carboxylates on the

DOI: 10.1021/jacs.9b02004
J. Am. Chem. Soc. XXXX, XXX, XXX−XXX

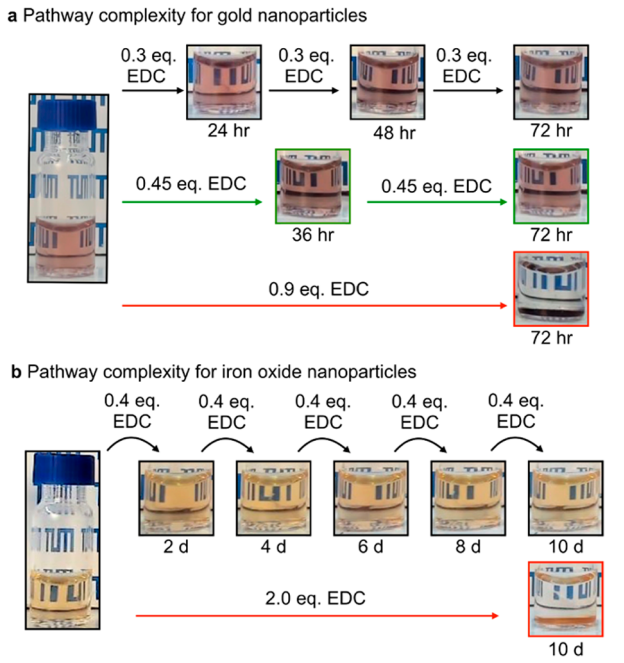

Figure 6. (a) Pathway complexity in the EDC-driven reaction cycle involving gold- (a) or iron oxide- (b) based nanoparticles as a precursor.

particle to their corresponding NHS-esters. With small amounts of EDC, the nanoparticles are activated, but to an insufficient degree for self-assembly. When more EDC is added, the gold or iron oxide nanoparticles assemble dissipatively driven by the reaction cycle; that is, they assemble and disassemble after EDC has been depleted. In contrast, when a large amount of EDC is added, the nanoparticles form large assemblies that remain kinetically trapped. The notion of a fuel-dependent kinetic trap implies that the behavior of the system is prone to pathway complexity; that is, the final position of the gold and iron oxide nanoparticles in their free energy landscape may depend on the preparative pathway. Indeed, we find that, when a large amount of EDC is added in small batches, it does not result in a kinetically trapped state. In contrast, when the same amount of EDC is added at once, it results in the irreversible kinetic trapping of the assemblies. In other words, two solutions of gold or iron oxide nanoparticles that are of the same final compositions (buffer, pH, temperature, reagents, and products) but have a different preparative history can result in different states in the energy landscape. The associated material properties are thus also dependent on sample history. To further develop supramolecular materials with complexity and sophistication as observed in living materials, an understanding of the relations between energy landscapes, material properties, and pathways complexity is fundamental.

■ ASSOCIATED CONTENT

Supporting Information

The Supporting Information is available free of charge on the ACS Publications website at DOI: 10.1021/jacs.9b02004.

Materials and methods, DLS data, TEM, SEM, and FTIR spectra, titration data (PDF)

■ AUTHOR INFORMATION

Corresponding Author

*job.boekhoven@tum.de

ORCID

Bernhard Rieger: 0000-0002-0023-884X

Job Boekhoven: 0000-0002-9126-2430

Funding

Deutsche Forschungsgemeinschaft via the International Research Training Group ATUMS (IRTG 2022) European Union Seventh Framework Programme under Grant No. 291763.

Notes

The authors declare no competing financial interest.

■ ACKNOWLEDGMENTS

R.K.G., B.R., M.S., and J.B. are grateful for funding from the Deutsche Forschungsgemeinschaft via the International Research Training Group ATUMS (IRTG 2022). C.W. is grateful for funding from the Deutsche Forschungsgemeinschaft through Transregional Collaborative Research Center (SFB/Transregio) 235 Project 16. J.B. is grateful for funding by the Technical University of Munich−Institute for Advanced Study, funded by the German Excellence Initiative and the European Union Seventh Framework Programme under Grant No. 291763. A.A. acknowledges funding from Studienstiftung des Deutschen Volkes.

■ REFERENCES

(1) Amabilino, D. B.; Smith, D. K.; Steed, J. W. Supramolecular materials. *Chem. Soc. Rev.* **2017**, *46* (9), 2404−2420.

(2) Stupp, S. I.; LeBonheur, V. V.; Walker, K.; Li, L. S.; Huggins, K. E.; Keser, M.; Amstutz, A. Supramolecular Materials: Self-Organized Nanostructures. *Science* **1997**, *276* (5311), 384−9.

(3) Aida, T.; Meijer, E. W.; Stupp, S. I. Functional supramolecular polymers. *Science* **2012**, *335* (6070), 813−7.

(4) Lampel, A.; McPhee, S. A.; Park, H. A.; Scott, G. G.; Humagain, S.; Hekstra, D. R.; Yoo, B.; Frederix, P.; Li, T. D.; Abzalimov, R. R.; Greenbaum, S. G.; Tuttle, T.; Hu, C.; Bettinger, C. J.; Ulijn, R. V. Polymeric peptide pigments with sequence-encoded properties. *Science* **2017**, *356* (6342), 1064−1068.

(5) Israelachvili, J. N.; Mitchell, D. J.; Ninham, B. W. Theory of self-assembly of hydrocarbon amphiphiles into micelles and bilayers. *J. Chem. Soc., Faraday Trans. 2* **1976**, *72*, 1525−1568.

(6) van Esch, J. H.; Feringa, B. L. New Functional Materials Based on Self-Assembling Organogels: From Serendipity towards Design. *Angew. Chem., Int. Ed.* **2000**, *39* (13), 2263−2266.

(7) Hartgerink, J. D.; Beniash, E.; Stupp, S. I. Self-assembly and mineralization of peptide-amphiphile nanofibers. *Science* **2001**, *294* (5547), 1684−8.

(8) Mirkin, C. A.; Letsinger, R. L.; Mucic, R. C.; Storhoff, J. J. A DNA-based method for rationally assembling nanoparticles into macroscopic materials. *Nature* **1996**, *382* (6592), 607−9.

(9) Zhang, S. Fabrication of novel biomaterials through molecular self-assembly. *Nat. Biotechnol.* **2003**, *21* (10), 1171−8.

(10) Alakpa, E. V.; Jayawarna, V.; Lampel, A.; Burgess, K. V.; West, C. C.; Bakker, S. C. J.; Roy, S.; Javid, N.; Fleming, S.; Lamprou, D. A.; Yang, J.; Miller, A.; Urquhart, A. J.; Frederix, P. W. J. M.; Hunt, N. T.; Péault, B.; Ulijn, R. V.; Dalby, M. J. Tunable Supramolecular Hydrogels for Selection of Lineage-Guiding Metabolites in Stem Cell Cultures. *Chem.* **2016**, *1* (2), 298−319.

(11) Silva, G. A.; Czeisler, C.; Niece, K. L.; Beniash, E.; Harrington, D. A.; Kessler, J. A.; Stupp, S. I. Selective differentiation of neural progenitor cells by high-epitope density nanofibers. *Science* **2004**, *303* (5662), 1352−5.

DOI: 10.1021/jacs.9b02004
J. Am. Chem. Soc. XXXX, XXX, XXX−XXX

(12) Panettieri, S.; Ulijn, R. V. Energy landscaping in supramolecular materials. *Curr. Opin. Struct. Biol.* **2018**, *51*, 9−18.
(13) Sorrenti, A.; Leira-Iglesias, J.; Markvoort, A. J.; de Greef, T. F. A.; Hermans, T. M. Non-equilibrium supramolecular polymerization. *Chem. Soc. Rev.* **2017**, *46* (18), 5476−5490.
(14) Ogi, S.; Stepanenko, V.; Sugiyasu, K.; Takeuchi, M.; Wurthner, F. Mechanism of self-assembly process and seeded supramolecular polymerization of perylene bisimide organogelator. *J. Am. Chem. Soc.* **2015**, *137* (9), 3300−7.
(15) Tantakitti, F.; Boekhoven, J.; Wang, X.; Kazantsev, R. V.; Yu, T.; Li, J.; Zhuang, E.; Zandi, R.; Ortony, J. H.; Newcomb, C. J.; Palmer, L. C.; Shekhawat, G. S.; de la Cruz, M. O.; Schatz, G. C.; Stupp, S. I. Energy landscapes and functions of supramolecular systems. *Nat. Mater.* **2016**, *15* (4), 469−76.
(16) Korevaar, P. A.; Newcomb, C. J.; Meijer, E. W.; Stupp, S. I. Pathway selection in peptide amphiphile assembly. *J. Am. Chem. Soc.* **2014**, *136* (24), 8540−3.
(17) Merindol, R.; Loescher, S.; Samanta, A.; Walther, A. Pathway-controlled formation of mesostructured all-DNA colloids and superstructures. *Nat. Nanotechnol.* **2018**, *13* (8), 730−738.
(18) Leira-Iglesias, J.; Sorrenti, A.; Sato, A.; Dunne, P. A.; Hermans, T. M. Supramolecular pathway selection of perylenediimides mediated by chemical fuels. *Chem. Commun.* **2016**, *52* (58), 9009−9012.
(19) van Rossum, S. A. P.; Tena-Solsona, M.; van Esch, J. H.; Eelkema, R.; Boekhoven, J. Dissipative out-of-equilibrium assembly of man-made supramolecular materials. *Chem. Soc. Rev.* **2017**, *46* (18), 5519−5535.
(20) De, S.; Klajn, R. Dissipative Self-Assembly Driven by the Consumption of Chemical Fuels. *Adv. Mater.* **2018**, *30* (41), No. e1706750.
(21) Grötsch, R. K.; Boekhoven, J. Unique properties of supramolecular biomaterials through nonequilibrium self-assembly. In *Self-assembling Biomaterials;* Silva, R. M. P. D., Azevedo, H. S., Eds.; Woodhead Publishing, 2018; pp 235−250.
(22) Boekhoven, J.; Hendriksen, W. E.; Koper, G. J.; Eelkema, R.; van Esch, J. H. Transient assembly of active materials fueled by a chemical reaction. *Science* **2015**, *349* (6252), 1075−9.
(23) Debnath, S.; Roy, S.; Ulijn, R. V. Peptide nanofibers with dynamic instability through nonequilibrium biocatalytic assembly. *J. Am. Chem. Soc.* **2013**, *135* (45), 16789−92.
(24) Maiti, S.; Fortunati, I.; Ferrante, C.; Scrimin, P.; Prins, L. J. Dissipative self-assembly of vesicular nanoreactors. *Nat. Chem.* **2016**, *8* (7), 725−31.
(25) Tena-Solsona, M.; Wanzke, C.; Riess, B.; Bausch, A. R.; Boekhoven, J. Self-selection of dissipative assemblies driven by primitive chemical reaction networks. *Nat. Commun.* **2018**, *9* (1), 2044.
(26) Tena-Solsona, M.; Riess, B.; Grötsch, R. K.; Lohrer, F. C.; Wanzke, C.; Kasdorf, B.; Bausch, A. R.; Muller-Buschbaum, P.; Lieleg, O.; Boekhoven, J. Non-equilibrium dissipative supramolecular materials with a tunable lifetime. *Nat. Commun.* **2017**, *8*, 15895.
(27) Rieß, B.; Boekhoven, J. Applications of Dissipative Supramolecular Materials with a Tunable Lifetime. *Chem. Nano Mat* **2018**, *4* (8), 710−719.
(28) Heuser, T.; Steppert, A. K.; Molano Lopez, C.; Zhu, B.; Walther, A. Generic concept to program the time domain of self-assemblies with a self-regulation mechanism. *Nano Lett.* **2015**, *15* (4), 2213−9.
(29) Kundu, P. K.; Samanta, D.; Leizrowice, R.; Margulis, B.; Zhao, H.; Borner, M.; Udayabhaskararao, T.; Manna, D.; Klajn, R. Light-controlled self-assembly of non-photoresponsive nanoparticles. *Nat. Chem.* **2015**, *7* (8), 646−52.
(30) Leira-Iglesias, J.; Tassoni, A.; Adachi, T.; Stich, M.; Hermans, T. M. Oscillations, travelling fronts and patterns in a supramolecular system. *Nat. Nanotechnol.* **2018**, *13* (11), 1021−1027.
(31) Grötsch, R. K.; Angı, A.; Mideksa, Y. G.; Wanzke, C.; Tena-Solsona, M.; Feige, M. J.; Rieger, B.; Boekhoven, J. Dissipative Self-Assembly of Photoluminescent Silicon Nanocrystals. *Angew. Chem., Int. Ed.* **2018**, *57* (44), 14608−14612.
(32) van Ravensteijn, B. G. P.; Hendriksen, W. E.; Eelkema, R.; van Esch, J. H.; Kegel, W. K. Fuel-Mediated Transient Clustering of Colloidal Building Blocks. *J. Am. Chem. Soc.* **2017**, *139* (29), 9763−9766.
(33) Sawczyk, M.; Klajn, R. Out-of-Equilibrium Aggregates and Coatings during Seeded Growth of Metallic Nanoparticles. *J. Am. Chem. Soc.* **2017**, *139* (49), 17973−17978.
(34) Delamarche, E.; Michel, B.; Gerber, C.; Anselmetti, D.; Guentherodt, H. J.; Wolf, H.; Ringsdorf, H. Real-Space Observation of Nanoscale Molecular Domains in Self-Assembled Monolayers. *Langmuir* **1994**, *10* (9), 2869−2871.
(35) Totaro, K. A.; Liao, X.; Bhattacharya, K.; Finneman, J. I.; Sperry, J. B.; Massa, M. A.; Thorn, J.; Ho, S. V.; Pentelute, B. L. Systematic Investigation of EDC/sNHS-Mediated Bioconjugation Reactions for Carboxylated Peptide Substrates. *Bioconjugate Chem.* **2016**, *27* (4), 994−1004.
(36) Riess, B.; Wanzke, C.; Tena-Solsona, M.; Grötsch, R. K.; Maity, C.; Boekhoven, J. Dissipative assemblies that inhibit their deactivation. *Soft Matter* **2018**, *14* (23), 4852−4859.
(37) Klajn, R.; Bishop, K. J. M.; Grzybowski, B. A. Light-controlled self-assembly of reversible and irreversible nanoparticle supra-structures. *Proc. Natl. Acad. Sci. U. S. A.* **2007**, *104* (25), 10305.
(38) Song, G.; Li, J.; Yuan, Y.; Yao, L.; Gu, J.; Liu, Q.; Zhang, W.; Su, Y.; Zhang, D. Large-Area 3D Hierarchical Superstructures Assembled from Colloidal Nanoparticles. *Small* **2019**, *15* (18), 1805308.
(39) Heinen, L.; Walther, A. Temporal control of i-motif switch lifetimes for autonomous operation of transient DNA nanostructures. *Chemical Science* **2017**, *8* (5), 4100−4107.

DOI: 10.1021/jacs.9b02004
J. Am. Chem. Soc. XXXX, XXX, XXX−XXX